

# Disk-shaped bicelles in block copolymer/homopolymer blends

M. J. Greenall

*Institute of Mathematics, Physics and Computer Science,  
Physical Sciences Building, Aberystwyth University,  
Aberystwyth SY23 3BZ, United Kingdom.\**

## Abstract

Mixtures of micelle-forming and lamella-forming amphiphiles in solution can form disk-shaped bilayers, sometimes referred to as bicelles. Using self-consistent field theory (SCFT), we investigate the structure and stability of these aggregates in a blend of two species of PS-PDMS diblock with PDMS homopolymer at 225°C. We find that the center of each disk is mainly composed of lamella-forming diblocks, while its thicker rim is mostly formed of micelle-forming diblocks. However, this segregation is not perfect, and the concentration of micelle formers is of the order of 10% on the flat central surface of the bicelle. We also find that the addition of micelle former to the mixture of lamella former and homopolymer is necessary for disk-like bicelles to be stable. Specifically, the free energy density of the disk has a minimum as a function of the disk radius when both micelle- and lamella-forming diblocks are present, indicating that the bicelles have a preferred, finite radius. However, it decays monotonically when only lamella former is present, indicating that the bicelle structure is always unstable with respect to further aggregation in these systems. Finally, we identify a concentration range where the bicelle is predicted to have a lower free energy density than the simple cylindrical and lamellar aggregates, and so might be thermodynamically stable.

PACS numbers:

---

\*School of Mathematics and Physics, University of Lincoln, Brayford Pool, Lincoln LN6 7TS, United Kingdom.; Electronic address: mjgreenall@physics.org

## I. INTRODUCTION

Mixtures of lamella-forming and micelle-forming amphiphiles can form structures in solution that are not seen when only one type of amphiphile is present [1–3]. These structures, which include disks, ribbons, and perforated lamellae [4, 5], have been studied in particular depth in lipid-detergent mixtures, where they are known collectively as *bicelles* [6]. Bicelles are widely used in biophysical experiments as model membranes [4] for the solubilization of proteins [7, 8], and have several advantages over alternative membrane structures such as multilayers and micelles. In particular, they avoid the curvature and strain effects that can occur in micelles [9, 10], and, unlike oriented multilayers, are usually optically transparent [11]. They contain smaller amounts of detergent, which can be harmful to membrane proteins, than mixed micelles [8], and, under certain circumstances [4, 12–15], can be aligned in a magnetic field. Which of the various bicellar morphologies forms depends on a variety of factors [16], with the disk morphology appearing at lower temperatures [17] and lower lamella-former concentrations [4], and perforated lamellae forming at higher temperatures [17] and higher concentrations of lamella former [4].

Much progress has also been made in the modeling of bicelles, using techniques ranging from simple geometric models [18] to microscopic simulations [19]. Recently, a theory based on the chemical potentials of the amphiphiles in differently shaped aggregates has been used to model light-scattering data on disk formation in mixed surfactant systems [20]. Disk-shaped bilayers and ribbon-like structures have been found in coarse-grained molecular dynamics simulations [19, 21–23], and similar techniques have been used to investigate the transformation of small vesicles into disks [24, 25] and vice versa [26]. However, the complexity of lipid-detergent systems, and the simplifying assumptions that must be made when modeling them, mean that detailed comparison of theoretical models with experimental results can prove difficult.

Fortunately, it can sometimes be possible to perform more detailed comparisons of theory with experiment for the self-assembly of micelles and bilayers in systems that are composed of a diblock copolymer and a homopolymer, rather than a lipid or detergent dissolved in water [27–30]. In these systems, scaling theories [28, 29] and self-consistent field theory [31] give a good description of the size of the micelles, and self-consistent field theory can also predict the shape of the aggregates that will be formed for a given set of polymer parameters

[32].

In the current paper, we take a similar approach to the study of disk-shaped bicelles, and use self-consistent field theory [33] to investigate the structures formed in a blend of two types of poly(styrene)-poly(dimethylsiloxane) (PS-PDMS) copolymer with poly(dimethylsiloxane) (PDMS) homopolymer. We have a number of reasons for focusing on this system. First, the two polymers segregate strongly [34, 35], with the result that the system will mimic the lower temperatures where the disk-shaped bicelle morphology is most likely to be seen. Second, the large difference in electron absorption and scattering of PS and PDMS means that the microstructures formed in this system can be studied directly by electron microscopy, without the need for staining [36]. The third reason is the possibility of modifying the properties of the PDMS. The two polymers have very different glass transition temperatures [37, 38], and the PS blocks will become glassy when the system is cooled to room temperature, while the PDMS will remain viscoelastic, yielding a dispersion of hard disks. Such systems [39] can display a range of behavior, including shear-induced phase separation [40] and the formation of networks of platelets [41, 42].

The paper is organized as follows. In the following section, we describe our PDMS/PS system. Next, we give a brief introduction to the technique to be used, self-consistent field theory (SCFT). We then present and discuss our results, and give our conclusions in the final section.

## II. DETAILS OF THE SYSTEM

As discussed in the Introduction, blends of PS and PDMS are strongly segregated, and the Flory  $\chi$  parameter between the two species is high. It is given as a function of temperature  $T$  (measured in K) by [34, 35]  $3.1 \times 10^{-2} + 58/T$ . This expression for  $\chi$  is defined with respect to a reference volume of  $1/\rho_0 = 100\text{\AA}^3$ , and is valid for temperatures from 165 to 225°C. To keep our SCFT algorithm numerically stable, we carry out our calculations at the upper end of this range (225°C), where the polymers will be slightly more weakly segregated and the interfaces less sharp. The lamella-forming species is chosen to have a PDMS block of molar mass 6000g/mol and a PS block of 13000g/mol, and the molar mass of the PDMS homopolymer is set to 4500g/mol. The homopolymer has been chosen to be shorter than the PDMS block of the copolymer to ensure thermodynamic stability [29, 43], and the ratio

of the block lengths of the copolymer has been set so that this species will have a strong tendency to form lamellae [32, 44]. A polymer chain with ‘hydrophobic’ and ‘hydrophilic’ components in a ratio of roughly two to one, as is the case here, also provides a simple model of the long-chain DMPC molecules that form the body of bicelles in lipid-detergent mixtures [4, 19]. To ensure that it has a clear preference for forming micelles, the other species has a long PDMS block, with molar mass 24000g/mol, and a PS block of 6000g/mol. The overall weight fraction of copolymer, including both species, is set to 2.5%. Using this relatively low concentration has two advantages. First, it will allow us to neglect interactions between the aggregates when modeling the thermodynamics of the system. Second, it will avoid interference between the aggregate and the boundary of the calculation box. We do not risk dropping below the critical micelle concentration by using a copolymer concentration of this magnitude, because the system under consideration is very strongly segregated[27]. We also need to know the mean-square end-to-end distance,  $r_0^2$ , of each polymer species as a function of its molar mass,  $M$ . For polymers in a melt, this is given by an expression of the form  $r_0^2 \propto M$ , where the ratio  $r_0^2/M$  is close to constant for a given polymer [45]. For PS [45], we have that  $r_0^2/M \approx 0.49$ . The dimensions of PDMS [46] are rather similar, and  $r_0^2/M \approx 0.53$ .

Certain of the parameters above cannot be used directly as input to an SCFT calculation, and need to be converted into the appropriate forms. First, the molar masses listed above are converted to molar volumes [27] using the specific volumes (in  $\text{cm}^3/\text{g}$ ) of PS and PDMS. Empirical expressions for the specific volumes of PS [47] and PDMS [48] as a function of temperature are taken from the literature. The molar volumes are then used to calculate the volume fraction of PDMS in each type of diblock and the volume ratios of the various species. The overall weight fraction of diblocks is converted to a volume fraction by a similar procedure, and the volume of a single molecule of each species in  $\text{\AA}^3$  is calculated by dividing the appropriate molar volume by 0.60221413, a numerical constant that incorporates Avogadro’s number and the conversion from  $\text{cm}^3$  to  $\text{\AA}^3$ . Finally, the number,  $N$ , of repeat units in a polymer chain can be calculated by dividing the volume of the molecule by the reference volume,  $1/\rho_0$ .

### III. SELF-CONSISTENT FIELD THEORY

Self-consistent field theory (SCFT) [33] is a mean-field model that has been used with success to calculate the form and free energy of equilibrium [49–51] and metastable [52, 53] structures in systems composed of homopolymers [54], copolymers [55, 56] and mixtures of these [57]. SCFT has several features that make it especially suited to the current problem. First, as stated above, it has been shown to give a good description of the shape and size of micelles in blends of a single species of block copolymer with a homopolymer [31, 32], a system closely related to the current one. Second, it is faster than simulation techniques such as Monte Carlo, but can yield comparably accurate predictions of micelle size and shape [58–60]. This will allow bicelles of a range of sizes to be studied in a reasonable period of time. Finally, it does not require any assumptions to be made regarding the segregation of copolymers of different architecture within an aggregate, meaning that any such effects that we observe are a natural prediction of the theory and have not been added by hand.

We now give a short overview of the application of SCFT to our system of two copolymers and a homopolymer, and refer the reader to reviews [51, 61, 62] for in-depth presentations of the theory and to earlier papers [31, 32, 63] for a detailed description of our calculations. SCFT is a coarse-grained theory, and individual molecules are modeled as random walks in space [62]. An ensemble of many such molecules is considered, and the intermolecular forces are modeled by introducing contact potentials between the molecules and assuming that the blend is incompressible [51]. The Flory  $\chi$  parameter discussed above is used to specify the strength of the repulsion between the two chemical species. In order to reduce the computational difficulty of the problem, fluctuations are neglected; that is, a mean-field approximation is made [51]. In the case of long molecules, this approximation is quantitatively accurate [51, 58, 61].

SCFT can be used to perform calculations in different thermodynamical ensembles [52, 64]. In this paper, we perform all calculations in the canonical ensemble, which corresponds to keeping the amounts of copolymer and homopolymer in the simulation box fixed. This approach makes it easier for us to access more complex aggregates, such as bicelles. Such structures are more difficult to find in ensembles where the concentrations of the various species are able to change, and sometimes need to be stabilized by applying geometric constraints to the density profile [53].

Applying the mean-field approximation[51] to our system, we find that the SCFT expression for the free energy of a system of copolymer species 1 and 2 in homopolymer is given by

$$\begin{aligned} \frac{FN_1}{k_B T \rho_0 V} = & \frac{F_H N_1}{k_B T \rho_0 V} \\ & - (\chi N/V) \int d\mathbf{r} [(\phi_{\text{PDMS1}}(\mathbf{r}) + \phi_{\text{PDMS2}}(\mathbf{r}) + \phi_{\text{hPDMS}}(\mathbf{r}) - \bar{\phi}_{\text{PDMS1}} - \bar{\phi}_{\text{PDMS2}} - \bar{\phi}_{\text{hPDMS}}) \\ & \times (\phi_{\text{PS1}}(\mathbf{r}) + \phi_{\text{PS2}}(\mathbf{r}) - \bar{\phi}_{\text{PS1}} - \bar{\phi}_{\text{PS2}})] - (\bar{\phi}_{\text{PDMS1}} + \bar{\phi}_{\text{PS1}}) \ln(Q_1/V) \\ & - [(\bar{\phi}_{\text{PDMS2}} + \bar{\phi}_{\text{PS2}})/\alpha] \ln(Q_2/V) - (\bar{\phi}_{\text{hPDMS}}/\alpha_h) \ln(Q_h/V) \end{aligned} \quad (1)$$

where the  $\bar{\phi}_i$  are the mean volume fractions of the various components, with  $i = \text{PDMS1}$  or  $\text{PDMS2}$  for the poly(dimethyl siloxane) components of species 1 and 2,  $i = \text{PS1}$  or  $\text{PS2}$  for the poly(styrene) components and  $i = \text{hPDMS}$  for the homopolymer solvent, and the  $\phi_i(\mathbf{r})$  are the local volume fractions.  $V$  is the total volume,  $N_1$  is the number of repeat units in species 1, and  $F_H$  is the SCFT free energy of a homogeneous system of the same composition. The architectures of the individual molecules enter through the single-chain partition functions  $Q_{j=1,2,h}$ , which are calculated from the propagators  $q$  and  $q^\dagger$  [51]. These latter quantities satisfy diffusion equations with a field term that incorporates the polymer interactions. One field is associated with the PDMS segments, and one with the PS segments. This means that, to calculate the copolymer partition functions,  $Q_1$  and  $Q_2$ , the diffusion equation must be solved with the field appropriate to each of the two blocks of the copolymer [51, 61]. In addition, the difference between the expressions for the mean-square end-to-end distances of PDMS and PS [45, 46] must be taken into account when calculating the prefactor of the  $\nabla^2 q$  term in each block. The polymer density profiles are computed from integrals over the propagators [51, 61], with the volume fractions of PS and PDMS in each copolymer species entering via the limits of integration.

We perform all our calculations in cylindrical polar coordinates. Since we mainly focus on disk-shaped aggregates, we reduce the problem to a two-dimensional one by assuming that the system has rotational invariance about the  $z$ -axis, and carry out all our calculations in a cylindrical box. We impose reflecting boundary conditions at all edges of the box, and the center of the bicelle lies at the origin of the coordinate system. The vertical height of this box is set to  $Z = 450\text{\AA}$  (meaning that its effective height is  $900\text{\AA}$ ), and its radius  $R$  is varied according to a procedure that will be described later. The diffusion equations are

solved using a finite difference method [65] with a step size of  $2.5\text{\AA}$ . The curve parameter  $s$  that specifies the distance along the polymer backbone [61] runs from 0 to 1, and its step size is set to  $1/800$  for the copolymers and  $1/100$  for the homopolymer.

The derivation of the mean-field free energy  $F$  also yields a set of simultaneous equations relating the fields  $w_{\text{PDMS}}(\mathbf{r})$  and  $w_{\text{PS}}(\mathbf{r})$  to the densities  $\phi_i(\mathbf{r})$ . To calculate the density profiles for a given set of mean volume fractions  $\bar{\phi}_i$ , we make an initial guess for the fields that has the approximate form of the structure we wish to study, and then solve the diffusion equations to calculate the propagators and density profiles corresponding to these fields. The new  $\phi_i(\mathbf{r})$  are then substituted into the simultaneous equations to compute updated fields [66], which are then used in turn to compute new  $\phi_i(\mathbf{r})$  by solving the diffusion equation as described above. For the algorithm to remain stable, the iteration needs to be damped, and, instead of using the updated values of  $w_i$  directly to calculate the  $\phi_i$ , we use the linear combination  $\lambda w_i^{\text{new}} + (1-\lambda)w_i^{\text{old}}$  where  $\lambda \approx 0.04$ . This process is repeated until convergence is achieved. For smaller systems, this *simple mixing* is sufficient. However, in larger calculation boxes, it can stall after an initial period of convergence. When performing calculations on these systems, we follow Thompson and co-workers [67] in passing the fields generated by the simple mixing iterations to an Anderson mixing algorithm [68]. This algorithm has greater flexibility in the iteration steps it can take, since it stores a history of previous values of the  $w_i(\mathbf{r})$ , and calculates the next estimate for the fields by adding these together in a linear combination [69]. The pure Anderson mixing procedure is not stable in our case, and has to be damped [70, 71]. We find that a history of 50–100 previous values of the  $w_i(\mathbf{r})$  and damping parameter of 0.1–0.2 yield good results.

We now need to address the issue of how to relate the thermodynamics of a single bicelle to those of a larger system containing many aggregates. To do this, we adapt a procedure that has been developed to study simple micelles and bilayers [31, 32, 72, 73]. First, we compute the free-energy density of a cylindrical box containing a single disk-shaped aggregate. Since the copolymer concentration is low, the aggregate is surrounded by a large volume of homopolymer, and the shape of the aggregate is not influenced by contact with the boundaries of the system. The radius of the simulation box is then varied, keeping the total volume fractions of both types of copolymer constant. Changing the size of the box in this way causes the bicelle to grow in the radial direction. The free-energy density of the system is calculated for each box radius. As is the case when this method is applied to

micelles, there will be a minimum in the free energy as a function of the radius[73] if the bicelle is stable. This solution of the SCFT equations corresponds to the optimum size of the bicelle. If, on the other hand, the bicelle is unstable with respect to further aggregation, the free energy density will decay monotonically as the box radius is increased, meaning that the bicelle can always move to a more energetically favorable state by growing in the radial direction, eventually forming an extended bilayer.

This approach is designed to mimic the behavior of a larger system (of fixed volume and fixed copolymer volume fraction) containing many bicelles. The reason for this is that this larger system minimizes its total free energy by changing the number of aggregates and hence the volume (‘box size’) occupied by each. Minimizing the free energy density in this way locates the bicelle that is the most energetically favorable and therefore the most likely to be observed in a sample containing many aggregates.

This minimum of the free-energy density with respect to the box size  $V$  corresponds to the absolute free energy minimum of a solution of aggregates, and a point on the curve  $F(V)/Vk_B T$  corresponds to a *monodisperse* solution of aggregates of a given size. In an earlier publication [72], we showed how to use these curves to take into account simple fluctuations around the free energy minimum and so calculate the width,  $\Delta$ , of the size distribution of aggregates in a system containing only one type of amphiphile. This was achieved by relating the curvature of  $F(V)/Vk_B T$  to the second derivative,  $\partial^2 f_p / \partial p^2$ , of the free energy  $f_p$  of an aggregate containing  $p$  molecules, which was then used [74] to calculate  $\Delta$  via  $1/\Delta^2 = (1/k_B T) \partial^2 f_p / \partial p^2$ . We began by writing down an expression for the free-energy density  $F/Vk_B T$  of a monodisperse system of aggregates, each containing  $p$  copolymers. This was given by

$$\frac{F}{Vk_B T} = (c - pc_p) \{ \ln[(c - pc_p)v_1/e] + f_1 \} + c_p f_p \quad (2)$$

where  $c$  is the number density of copolymers,  $c_p = 1/V$  is the number density of aggregates,  $f_1$  is the free energy of a copolymer in solution,  $f_p$  is the free energy of an aggregate of  $p$  copolymers,  $v_1 = N_1/\rho_0$  is the volume of a single copolymer, and first term arises from the entropy of the free copolymers in solution. We then noted that a single SCFT calculation finds the local minimum of the free energy density  $F/Vk_B T$  for an aggregate in a box of volume  $V$ . In the process, it determines the optimum number of molecules in the aggregate for this box size and so corresponds to minimizing  $F/Vk_B T$  with respect to  $p$  at a given



aggregate number density  $1/V$ . Varying  $V$  then yields the curve  $F(V)/Vk_BT$ , from which we can read off  $d^2[F/Vk_BT]/dV^2$ . Remembering that this derivative is evaluated along the line where  $\partial[F/Vk_BT]/\partial p|_V = 0$ , we found that

$$\frac{1}{\Delta^2} = \frac{1}{k_B T} \frac{\partial^2 f_p}{\partial p^2} = \frac{v_1}{v_a^2/(V^3 d^2 \tilde{F}/dV^2) - (\phi V - v_a)}, \quad (3)$$

where we have written  $\tilde{F} = Fv_1/Vk_BT$ ,  $v_a = pv_1$ , and converted the number density  $c$  to the volume fraction  $\phi$  to express  $\Delta$  in terms of quantities that are either input to or results of our SCFT calculations.

We now extend this calculation to a system containing two amphiphile species. As in the calculation above, we suppose that there is only one type of aggregate in the system. We make the further simplifying assumption that the number fractions of the two species in the aggregate are the same as the overall number fractions. This turns out to hold accurately in our numerical results, and allows us to write the free-energy density of the two-species system as

$$\begin{aligned} \frac{F}{Vk_B T} = & (\psi_1 c - \psi_1 p c_p) \{ \ln[(\psi_1 c - \psi_1 p c_p) v_1 / e] + f_{11} \} \\ & + (\psi_2 c - \psi_2 p c_p) \{ \ln[(\psi_2 c - \psi_2 p c_p) v_2 / e] + f_{12} \} + c_p f_p, \end{aligned} \quad (4)$$

where the number densities of species 1 and 2 are  $\psi_1 c$  and  $\psi_2 c$  respectively (so that  $\psi_1 + \psi_2 = 1$ ),  $f_{11}$  and  $f_{12}$  are the free energies of single copolymers of species 1 and 2 in solution, and  $v_2$  is the volume of a single copolymer of species 2. This assumption also allows us to write the number of copolymers in the aggregate as  $p = v_a/v_{\text{eff}}$ , where

$$v_{\text{eff}} = \frac{\phi_1 v_1}{\phi_1 + \phi_2 v_1 / v_2} + \frac{\phi_2 v_2}{\phi_1 v_2 / v_1 + \phi_2}. \quad (5)$$

The calculation then proceeds as before [72], and we find that

$$\frac{1}{\Delta^2} = \frac{1}{k_B T} \frac{\partial^2 f_p}{\partial p^2} = \frac{1}{v_1 (v_a/v_{\text{eff}})^2 / (V^3 d^2 \tilde{F}/dV^2) - [(\phi_1/v_1 + \phi_2/v_2)V - v_a/v_{\text{eff}}]}, \quad (6)$$

where, as before, we have converted number densities to volume fractions. The extra factor of  $v_1$  in equation 6 arises from the normalization of the free energy in equation 1.

To see if the bicelle is likely to form, we also need to compare its free energy density with those of other aggregates. If we can establish that, for a given concentration range, the bicelle has a lower free-energy density than the simple spherical, cylindrical and lamellar

aggregates, there is a clear possibility that it will form in this region. To calculate the free energy density of spherical micelles, we simply continue our calculations to smaller values of the calculation box radius until the disk-like bicelle shrinks to a sphere. It turns out that, for the systems considered here, where the  $\chi$  parameter is large and a high proportion of the polymers have a strong preference for forming lamellae, spherical micelles have much higher free-energy densities than the other aggregates. In consequence, we omit them from our results. The free energies of the optimum cylinder and lamella are found by a similar method to that described above [32]. These structures are assumed to be of infinite extent, so calculating their optimum free energies using SCFT is a one-dimensional problem, with the box size being varied in the  $r$ - and  $z$ -directions respectively [32]. For convenience, and for consistency with our earlier calculations, we perform these calculations using the same two-dimensional algorithm as before, but with the calculation box made very thin in the direction in which the density profiles do not vary.

#### IV. RESULTS AND DISCUSSION

We begin this section by demonstrating that the disk-like bicelle structure is a solution to the SCFT equations. Next, we investigate the dependence of the free energy density of the disk-like bicelle on its radius, to determine in which systems the bicelle has a preferred size. Finally, we compare the free energy of the bicelle to those of the simple cylindrical and lamellar structures for a range of concentrations of the two copolymer species, to find the range of parameters for which it might form in an experiment.

##### A. The disk-shaped bicelle morphology

In Figure 1, we show a ray-traced plot of the surface of a disk-like bicelle obtained as a solution to the SCFT equations in the PS/PDMS system described above. 30% by weight of diblocks are sphere formers, and 70% are lamella formers. The surface is defined as the locus of the points where the local solvent volume fraction  $\phi_s(\mathbf{r}) = 0.5$ , and has a biconcave disk shape reminiscent of a red blood cell.

We now investigate the distribution of the two species, and their hydrophilic and hydrophobic components, within the bicelle. In Figure 2a, we show radial cuts through the

volume fraction profiles of the various blocks that make up the bicelle. The division of the bicelle into a well defined “hydrophobic” PS core and “hydrophilic” PDMS corona is clearly visible, with the interface between the two regions being located at around  $r = 1080\text{\AA}$ . A marked difference in behavior between the sphere-forming and lamella-forming species is also seen. Specifically, the sphere formers are concentrated at the edge of the bicelle, with the volume fraction profile of their hydrophobic components being sharply peaked just before the core-corona interface, and their relatively long hydrophilic components stretching out into the solvent. This structure, in which the species with a preference for forming curved membranes segregates to the rim of the bicelle, is often sketched in the literature [11], and our results show that it can be reproduced in explicit calculations.

The curves in Figure 2b are cuts through the same volume fraction profiles in the  $z$ -direction. Again, clear core and corona regions can be seen. The difference between the two plots lies in the fact that the peak in the hydrophobic profile of the sphere-forming species just before the core-corona interface is markedly less pronounced in the  $z$ -direction, confirming the clear preference of the sphere formers for the bicelle rim. However, the presence of this peak, which attains a maximum height of 0.12, shows that the segregation of the sphere formers to the rim is not perfect, with an appreciable concentration of this species remaining near  $r = 0$ , particularly on the flat surface of the bicelle. Again, this result agrees with the pictorial model of bicelles often suggested in the biophysics literature [11].

## B. The preferred radius of the bicelle

Having shown that the bicelle exists as a solution to SCFT and investigated the distribution of the two copolymer species within it, we now study the dependence of its free energy density on its radius, with the aim of finding whether it has a preferred size. The size of the bicelle is varied by changing the calculation box radius as described above, and we plot its free energy density against the radius of its core. We focus on the core radius because this is the measure of micelle size that is most easily measured in experiment [44]. Since the interface between the core and the corona is sharp, all reasonable definitions of the core radius will yield similar values, and we define it here as the value of  $r$  at which the core and corona densities are equal, so that  $\phi_{\text{PS1}}(\mathbf{r}) + \phi_{\text{PS2}}(\mathbf{r}) = \phi_{\text{PDMS1}}(\mathbf{r}) + \phi_{\text{PDMS2}}(\mathbf{r})$ .

Figure 3a shows the results of this calculation for the system studied above, where 30%

by weight of all amphiphiles are sphere formers and 70% are lamella formers. The curve of the free energy density shows a clear minimum as a function of the bicelle radius, showing that the aggregate has a preferred size.

We can now use Equation 6 to estimate the relative polydispersity in the aggregation number of the micelle,  $\Delta/p$ . This is found to be approximately 20%, corresponding [72] to a relative polydispersity of around 10% in the bicelle radius. This demonstrates that significant size selection takes place in this system, with a clear preferred size for the bicelles.

### C. Concentration dependence

We now compare the free energy density of the bicelle with those of the cylindrical and lamellar morphologies over a range of concentrations. Since the bicelle is a hybrid structure that contains elements of both the lamella and the cylinder, we expect [19] that it will form at compositions around that at which the free energy densities of these two structures are the same. We therefore begin by locating this composition, and focus our attention on its vicinity. Figure 4 shows the results of these calculations. At higher weight fractions of sphere-forming amphiphile, the cylindrical micelle has the lowest free-energy density and the lamella has the highest. As the amount of sphere former is reduced, the free-energy density of the bicelle becomes the lowest of the three aggregates: it drops below that of the cylinder, while remaining below that of the lamella. As the weight fraction of sphere former is decreased further, the free-energy densities of the bicelle and lamella become closer, although they do not cross within the range of compositions that we are able to study. It is possible that the two quantities approach each other asymptotically as the amount of sphere former tends to zero. This is consistent with the growth in the bicelle radius seen as the amount of sphere former is reduced (Figure 5). As the bicelle becomes very large, it approaches the lamella in shape, and the free-energy densities of the two structures can also be expected to become very close.

## V. CONCLUSIONS

Using self-consistent field theory, we have studied the structure and stability of disk-like bicelles in a blend of lamella-forming and sphere-forming PS-PDMS diblocks with PDMS

homopolymer. We have found that these structures have a characteristic biconcave disk shape, like red blood cells. Furthermore, we have shown that the two amphiphile species are unequally distributed within the aggregate, with the center being mainly composed of lamella formers, and the rim being mostly formed of micelle formers. This picture of bicelles is often sketched in the biophysics literature [11], and is reproduced here in calculations on a well defined model.

We also find that the presence of micelle former is necessary for disk-like bicelles to be stable, and that they will be unstable with respect to further aggregation when only lamella former is present. Finally, we locate a region of parameter space range where the bicelle is predicted to have a lower free energy density than the competing cylindrical and lamellar aggregates.

There are a number of ways in which our calculations could be extended. First, we used the rather high temperature of 225°C in order to keep the  $\chi$  parameter at a level that our existing numerical methods were able to deal with. Further refinements of the Anderson mixing method and the algorithm used to solve the diffusion equation might allow the calculations to be extended to lower temperatures, where the concentration range at which the bicelle has a lower free-energy density than the other structures should be broader. Second, perhaps using these extended methods, we could look for other polymer blends in which the bicelle is predicted to be stable and in which its presence could have an effect on the mechanical properties. Finally, a similar SCFT approach could be applied to lipid systems [75], where bicelles were originally observed. This could be used to investigate the degree of detergent penetration into the center of the bicelle, an important issue for the biophysical experiments that use bicelles as model membranes.

- 
- [1] S. Jain and F. S. Bates, *Macromolecules* **37**, 1511 (2004).
  - [2] S. A. Safran, P. Pincus, and D. Andelman, *Science* **248**, 354 (1990).
  - [3] A. Zidovska, K. K. Ewert, J. Quispe, B. Carragher, C. S. Potter, and C. R. Safinya, *Langmuir* **25**, 2979 (2009).
  - [4] U. H. Dürr, R. Soong, and A. Ramamoorthy, *Prog. Nucl. Mag. Res. Sp.* **69**, 1 (2013).
  - [5] J. Katsaras, T. A. Harroun, J. Pencer, and M.-P. Nieh, *Naturwissenschaften* **92**, 355 (2005).

- [6] U. H. Dürr, M. Gildenberg, and A. Ramamoorthy, *Chem. Rev.* **112**, 6054 (2012).
- [7] C. R. Sanders and G. C. Landis, *Biochemistry* **34**, 4030 (1995).
- [8] A. M. Seddon, P. Curnow, and P. J. Booth, *Biochim. Biophys. Acta* **1666**, 105 (2004).
- [9] N. Matsumori and M. Murata, *Nat. Prod. Rep.* **27**, 1480 (2010).
- [10] R. S. Prosser, F. Evanics, J. L. Kitevski, and M. S. Al-Abdul-Wahid, *Biochemistry* **45**, 8453 (2006).
- [11] C. R. Sanders and R. S. Prosser, *Structure* **6**, 1227 (1998).
- [12] C. Loudet, A. Diller, A. Grélard, R. Oda, and E. J. Dufourc, *Prog. Lipid Res.* **49**, 289 (2010).
- [13] A. Diller, C. Loudet, F. Aussenac, G. Raffard, S. Fournier, M. Laguerre, A. Grélard, S. J. Opella, F. M. Marassi, and E. J. Dufourc, *Biochimie* **91**, 744 (2009).
- [14] P. M. Macdonald, Q. Saleem, A. Lai, and H. H. Morales, *Chem. Phys. Lipids* **166**, 31 (2013).
- [15] P. Ram and J. H. Prestegard, *Biochim. Biophys. Acta* **940**, 289 (1988).
- [16] C. Sanders, A. K. Hoffmann, D. N. Gray, M. H. Keyes, and C. D. Ellis, *ChemBioChem* **5**, 423 (2004).
- [17] J. Ramos, A. Imaz, J. Callejas-Fernández, L. Barbosa-Barros, J. Estelrich, M. Quesada-Pérez, and J. Forcada, *Soft Matter* **7**, 5067 (2011).
- [18] R. R. Vold and R. S. Prosser, *J. Magn. Reson. Ser. B* **113**, 267 (1996).
- [19] R. Vácha and D. Frenkel, *Langmuir* **30**, 4229 (2014).
- [20] S. E. Anachkov, P. A. Kralchevsky, K. D. Danov, G. S. Georgieva, and K. P. Ananthapadmanabhan, *J. Colloid Interf. Sci.* **416**, 258 (2014).
- [21] J. de Joannis, F. Y. Jiang, and J. T. Kindt, *Langmuir* **22**, 998 (2006).
- [22] H. Noguchi, *J. Chem. Phys.* **138**, 024907 (2013).
- [23] H. Lee and R. W. Pastor, *J. Phys. Chem. B* **115**, 7830 (2011).
- [24] W. Shinoda, T. Nakamura, and S. O. Nielsen, *Soft Matter* **7**, 9012 (2011).
- [25] H. Noguchi, *Soft Matter* **8**, 8926 (2012).
- [26] S. J. Marrink and A. E. Mark, *J. Am. Chem. Soc.* **125**, 15233 (2003).
- [27] D. J. Kinning, E. L. Thomas, and L. J. Fetters, *Macromolecules* **24**, 3893 (1991).
- [28] R.-J. Roe, *Macromolecules* **19**, 728 (1986).
- [29] L. Leibler, H. Orland, and J. C. Wheeler, *J. Chem. Phys.* **79**, 3550 (1983).
- [30] A. M. Mayes and M. O. de la Cruz, *Macromolecules* **21**, 2543 (1988).
- [31] M. J. Greenall, D. M. A. Buzza, and T. C. B. McLeish, *Macromolecules* **42**, 5873 (2009).

- [32] M. J. Greenall, D. M. A. Buzza, and T. C. B. McLeish, *J. Chem. Phys.* **131**, 034904 (2009).
- [33] S. F. Edwards, *Proc. Phys. Soc.* **85**, 613 (1965).
- [34] E. W. Cochran, D. C. Morse, and F. S. Bates, *Macromolecules* **36**, 782 (2003).
- [35] H. B. Eitouni and N. P. Balsara, *Physical Properties of Polymers Handbook* (Springer-Verlag, New York, 2007), chap. 19, 2nd ed.
- [36] J. C. Saam and F. W. G. Fearon, *Ind. Eng. Chem. Prod. Res. Develop.* **10**, 10 (1971).
- [37] W. W. Y. Chow, K. F. Lei, G. Shi, W. J. Li, and Q. Huang, *Smart Mater. Struct.* **15**, S112 (2006).
- [38] S. Krause, Z.-H. Lu, and M. Iskandar, *Macromolecules* **15**, 1076 (1982).
- [39] L. M. C. Dykes, J. M. Torkelson, W. R. Burghardt, and R. Krishnamoorti, *Polymer* **51**, 4916 (2010).
- [40] A. B. D. Brown and A. R. Rennie, *Chem. Eng. Sci.* **56**, 2999 (2001).
- [41] T. Nicolai and S. Cocard, *Eur. Phys. J. E* **5**, 221 (2001).
- [42] S. P. Patil, R. Mathew, T. G. Ajithkumar, P. R. Rajamohanan, T. S. Mahesh, and G. Kumaraswamy, *J. Phys. Chem. B* **112**, 4536 (2008).
- [43] A. M. Mayes and M. O. Delacruz, *Macromolecules* **21**, 2543 (1988).
- [44] D. J. Kinning, K. I. Winey, and E. L. Thomas, *Macromolecules* **21**, 3502 (1988).
- [45] J. Brandrup and E. H. Immergut, eds., *Polymer Handbook* (Wiley, New York, 1989).
- [46] T. Konishi, T. Yoshizaki, and H. Yamakawa, *Macromolecules* **24**, 5614 (1991).
- [47] M. J. Richardson and N. G. Savill, *Polymer* **18**, 3 (1977).
- [48] H. Shih and P. J. Flory, *Macromolecules* **5**, 758 (1972).
- [49] P. Maniadis, T. Lookman, E. M. Kober, and K. O. Rasmussen, *Phys. Rev. Lett.* **99**, 048302 (2007).
- [50] F. Drolet and G. H. Fredrickson, *Phys. Rev. Lett.* **83**, 4317 (1999).
- [51] M. W. Matsen, in *Soft Matter*, edited by G. Gompper and M. Schick (Wiley-VCH, Weinheim, 2006), chap. 2.
- [52] D. Duque, *J. Chem. Phys.* **119**, 5701 (2003).
- [53] K. Katsov, M. Müller, and M. Schick, *Biophys. J.* **87**, 3277 (2004).
- [54] A. Werner, M. Müller, F. Schmid, and K. Binder, *J. Chem. Phys.* **110**, 1221 (1999).
- [55] M. Müller and G. Gompper, *Phys. Rev. E* **66**, 041805 (2002).
- [56] J. F. Wang, K. K. Guo, L. J. An, M. Müller, and Z. G. Wang, *Macromolecules* **43**, 2037

- (2010).
- [57] N. A. Denesyuk and G. Gompper, *Macromolecules* **39**, 5497 (2006).
  - [58] A. Cavallo, M. Müller, and K. Binder, *Macromolecules* **39**, 9539 (2006).
  - [59] C. M. Wijmans and P. Linse, *Langmuir* **11**, 3748 (1995).
  - [60] F. A. M. Leermakers and J. M. H. M. Scheutjens, *J. Colloid Interface Sci.* **136**, 231 (1990).
  - [61] G. H. Fredrickson, *The Equilibrium Theory of Inhomogeneous Polymers* (Oxford University Press, Oxford, 2006).
  - [62] F. Schmid, *J. Phys.: Condens. Matter* **10**, 8105 (1998).
  - [63] M. J. Greenall and G. Gompper, *Langmuir* **27**, 3416 (2011).
  - [64] J. Zhou and A.-C. Shi, *Macromol. Theory Simul.* **20**, 690 (2011).
  - [65] W. H. Press, B. P. Flannery, S. A. Teukolsky, and W. T. Vetterling, *Numerical Recipes in C* (Cambridge University Press, Cambridge, 1992), 2nd ed.
  - [66] M. W. Matsen, *J. Chem. Phys.* **121**, 1938 (2004).
  - [67] R. B. Thompson, K. Ø. Rasmussen, and T. Lookman, *J. Chem. Phys.* **120**, 31 (2004).
  - [68] D. G. Anderson, *J. Assoc. Comput. Mach.* **12**, 547 (1965).
  - [69] K. C. Ng, *J. Chem. Phys.* **61**, 2680 (1974).
  - [70] F. Schmid, *Phys. Rev. E* **55**, 5774 (1997).
  - [71] P. Stasiak and M. W. Matsen, *Eur. Phys. J. E* **34**, 110 (2011).
  - [72] M. J. Greenall and C. M. Marques, *Phys. Rev. Lett* **110**, 088301 (2013).
  - [73] C. Y. Liaw, K. J. Henderson, W. R. Burghardt, J. Wang, and K. R. Shull, *Macromolecules* **48**, 173 (2015).
  - [74] S. Puvvada and D. Blankschtein, *J. Chem. Phys.* **92**, 3710 (1990).
  - [75] R. A. Kik, F. A. M. Leermakers, and J. M. Kleijn, *Phys. Rev. E* **81**, 021915 (2010).



## Figures

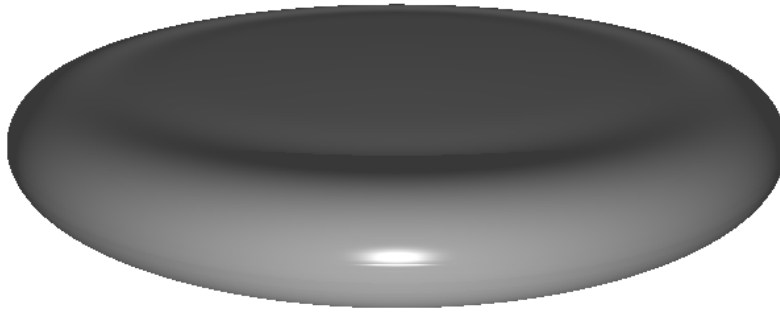


FIG. 1: Ray-traced plot of the surface of the bicelle.

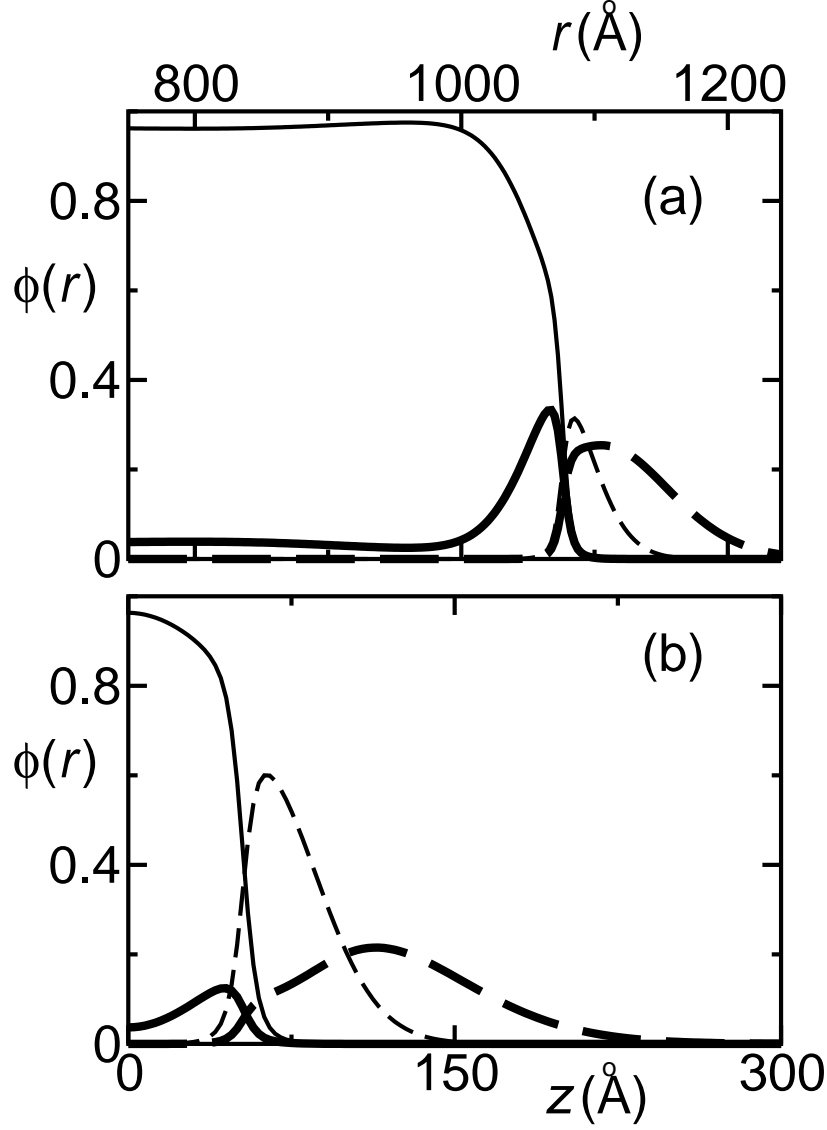


FIG. 2: Cuts through the volume fraction profiles of the various blocks making up the bicelle: sphere former PS blocks (thick solid line); sphere former PDMS blocks (thick dashed line); lamella former PS blocks (thin solid line); lamella former PDMS blocks (thin dashed line). The volume fraction profile of the PDMS homopolymer “solvent” is omitted for clarity. Panel (a) shows cuts in the  $r$ -direction, and panel (b) shows cuts in the  $z$ -direction. Note that neither panel shows the full range of the calculation box.

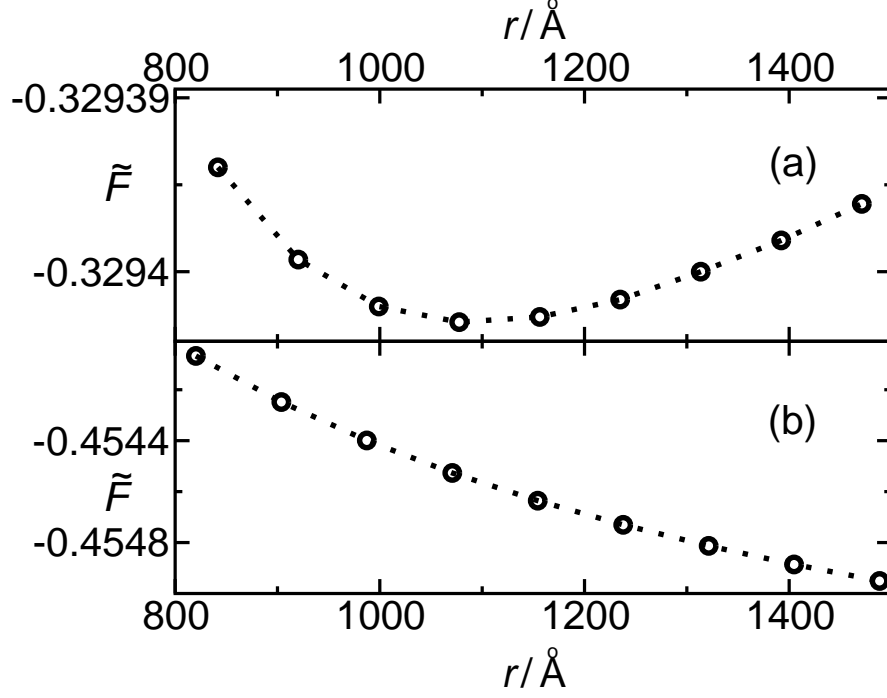


FIG. 3: Plots of the free-energy density against bicelle core radius for (a) a mixed system in which 30% by weight of all amphiphiles are sphere formers and 70% are lamella formers and (b) a pure system in which all amphiphiles are lamella formers. The narrow range of the  $\tilde{F}$  axes arises because the system is dilute and the free energy density is calculated for the entire calculation box, with the result that the differences in free energy density between one size of bicelle and another appear small. However, a more detailed calculation, in which the curvature of the free energy per chain in the bicelle is extracted from the above curves, reveals that the size selection in this system is significant, with a relative polydispersity,  $\Delta/p$ , of approximately 20% in the aggregation number, corresponding to a relative polydispersity of around 10% in the radius.

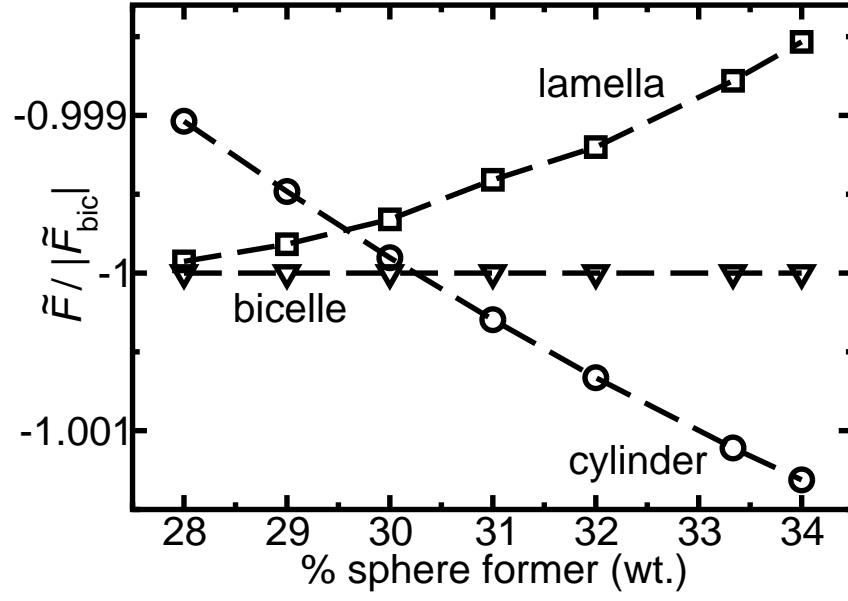


FIG. 4: Free energy densities of the lamella (squares), bicelle (triangles) and cylinder (circles), normalised with respect to that of the bicelle and plotted against the percentage of amphiphiles that are sphere formers.

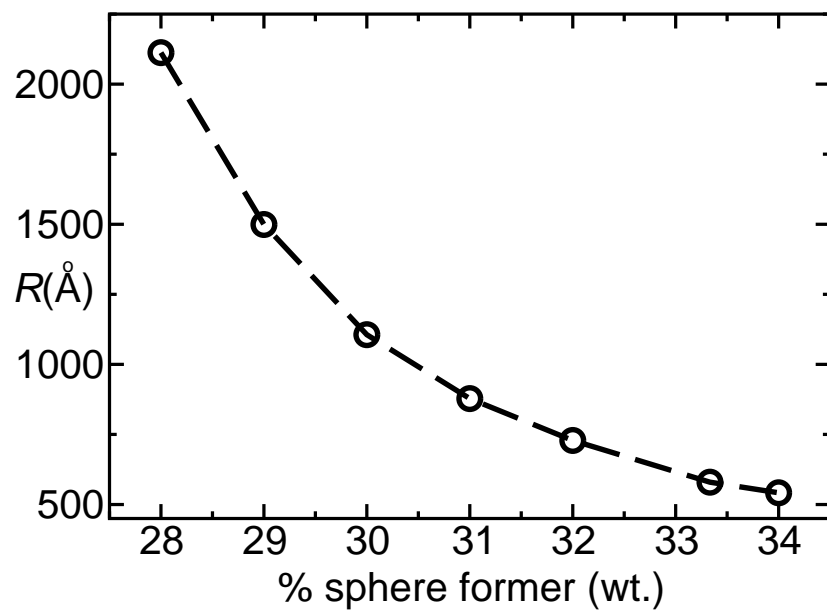


FIG. 5: The bicelle core radius plotted against the percentage of amphiphiles that are sphere formers.